Seizure Onset Detection Using Empirical Mode Decomposition and Common Spatial Pattern

Chaosong Li, Weidong Zhou, Guoyang Liu, Yanli Zhang, Minxing Geng, Zhen Liu, Shang Wang, and Wei Shang

***Abstract*— Automatic seizure onset detection plays an important role in epilepsy diagnosis. In this paper, a novel seizure onset detection method is proposed by combining empirical mode decomposition (EMD) of long-term scalp electroencephalogram (EEG) with common spatial pattern (CSP). First, wavelet transform (WT) and EMD are employed on EEG recordings respectively for filtering pre-processing and time-frequency decomposition. Then CSP is applied to reduce the dimension of multi-channel time-frequency representation, and the variance is extracted as the only feature. Afterwards, a support vector machine (SVM) group consisting of ten SVMs is served as a robust classifier. Finally, the post-processing is adopted to acquire a higher recognition rate and reduce the false detection rate. The results obtained from CHB-MIT database of 977 h scalp EEG recordings reveal that the proposed system can achieve a segment-based sensitivity of 97.34% with a specificity of 97.50% and an event-based sensitivity of 98.47% with a false detection rate of 0.63/h. This proposed detection system was also validated on a clinical scalp EEG database from the Second Hospital of Shandong University, and the system yielded a sensitivity of 93.67% and a specificity of 96.06%. At the event-based level, a sensitivity of 99.39% and a false detection rate of 0.64/h were obtained. Furthermore, this work showed that the CSP spatial filter was helpful to identify EEG channels involved in seizure onsets. These satisfactory results indicate that the proposed system may provide a reference for seizure onset detection in clinical applications.**

Manuscript received July 1, 2020; revised December 29, 2020; accepted January 25, 2021. Date of publication January 28, 2021; date of current version March 2, 2021. This work was supported in part by the Key Program of the Natural Science Foundation of Shandong Province under Grant ZR2020LZH009, in part by the Development Program of Science and Technology of Shandong under Grant 2014GSF118171, in part by the Research Funds of Science and Technology Innovation Committee of Shenzhen Municipality under Grant JCYJ20180305164357463, and in part by the National Natural Science Foundation of China under Grant 61801269. *(Corresponding author: Weidong Zhou.)*

Chaosong Li, Guoyang Liu, and Minxing Geng are with the School of Microelectronics, Shandong University, Jinan 250100, China (e-mail: lichaosong1995@163.com; virter1995@outlook.com; gengminxing1995@163.com).

Weidong Zhou is with the School of Microelectronics, Shandong University, Jinan 250100, China, and also with the Shenzhen Research Institute, Shandong University, Shenzhen 518057, China (e-mail: wdzhou@sdu.edu.cn).

Yanli Zhang is with the School of Information and Electronic Engineering, Shandong Technology and Business University, Yantai 264005, China (e-mail: sdlslily@163.com).

Zhen Liu, Shang Wang, and Wei Shang are with The Second Hospital of Shandong University, Jinan 250100, China (e-mail: 458292614@qq.com; wangshang009@126.com; wshang85@aliyun.com).

Digital Object Identifier 10.1109/TNSRE.2021.3055276

***Index Terms*— Seizure onset detection, scalp EEG, empirical mode decomposition, common spatial pattern.**

I. Introduction

EPILEPSY is one of the most common neurological disorder that affects more than 60 million people worldwide [1]. Electroencephalogram (EEG) records brain activities and has the ability to provide valuable guidance for epilepsy diagnosis [2]. Long-term EEG monitoring often lasts several hours or days, so the interpretation of these raw EEG data can become error-prone and time-consuming [3], [4]. Typically, an 18-channel, 36-h digital recording produces approximately 1.20 GB of data, which is equivalent to over 20 thousand pages of conventional paper EEG [5]. It is difficult to have enough neurologists available to review all EEGs, and the problem becomes worse as the number of channels increases [6], [7]. Additionally, the collected EEG signals always contain artifacts originating from various sources such as muscle activities, eye-blinks, and environment [8]. These artifacts greatly hinder the visual inspection of EEG by experts [9]. Automatic seizure onset detection, therefore, is highly in demand for clinical application.

The great progress for automatic seizure onset detection has been made in the past decades. Different EEG features based on time domain [10], [11], frequency domain [12]–[14] and nonlinear dynamics theory [15], [16] have been successively proposed. The automatic seizure onset detection system was first developed by Gotman [10] in 1980s. In his work, EEG signals were decomposed into half waves, and the peak amplitude, duration, slope, and sharpness were used as features. Zhang and Chen [12] utilized local mean decomposition (LMD) to obtain a series of product functions of EEG, and employed the temporal statistical and non-linear features based on time-frequency representation to characterize seizures. In the work of Kumar *et al.* [15], the fuzzy approximate entropy of each sub-band of discrete wavelet transform (DWT) was acquired as the feature to classify EEG signals. More recently, many techniques utilizing machine learning [17]–[19] were proposed to detect EEG signals. Al Ghayab *et al.* [19] combined the information in frequency domain, the information gain technique with a least square support vector machine (LS-SVM) for epilepsy detection.

Common spatial pattern (CSP) was originally proposed by Fukunaga [20] in 1974 and was applied to the field of EEG

analysis by Koles *et al.* [21]. It is a mathematical procedure that finds a spatial filter to project EEG segments onto a space so that its variance from one class is maximized while that from another class is minimized [22]. As a feature extraction algorithm, CSP is widely used including but not limited to electromyography (EMG) signal separation [23], [24], motor imagery [25], [26] and importance evaluation of independent components. However, CSP is relatively less explored in seizure onset detection [27]. Alotaiby *et al.* [28] fed CSP-based features into a linear discriminant analysis (LDA) classifier and adopted a leave-one-out cross-validation strategy to predict the onset of epilepsy in terms of each patient. There are obvious advantages for CSP in processing multi-channel EEGs, such as CSP can reduce data dimension automatically and extract spatial features of EEGs with lower computational burden.

Empirical mode decomposition (EMD) was first proposed by Huang *et al.* [29] in 1998. The EMD algorithm decomposes the signal into a finite number of Intrinsic Mode Functions (IMFs), relying on the time scale characteristics of signals, without pre-setting any basis function [30]. A lot of research has focused on feature extraction of EEG using the instantaneous frequency [31], [32] acquired from EMD. Martis *et al.* [31] fed the spectral energy, spectral entropy, and spectral peak from each IMF into a decision tree classifier for distinguishing seizures in EEG signals. Li *et al.* [32] captured the coefficient of variation and fluctuation index after EMD, as inputs into the SVM classifier.

This paper presents a novel seizure onset detection method based on EMD and CSP algorithm. The motivation behind the combination of CSP and EMD is to enhance the signal-to-noise ratio (SNR) of EEG signals by EMD and make up the defects of CSP such as the noise sensibility. The system described here consists of 4 steps. In the first step, we break down the multi-channel EEG into 2-s epochs and apply discrete wavelet transform (DWT) and EMD to each segment. After eliminating various artifacts, the second step devotes to the extraction of variance feature using CSP, which also be utilized to analyze which channels are involved in seizure onset. After classification in the third step, post-processing is employed to reduce the false detection rate. In this study, the results reveal two main advantages of our framework: low computational cost with only one feature, and the ability to help identify which brain regions are related to seizure onsets.

The remainder of this paper is organized as follows. Section 2 gives a brief description of the used scalp EEG databases. Section 3 is devoted to describe the proposed seizure onset detection method and Section 4 presents the evaluation results. Section 5 discusses the importance of EMD and CSP, and the performance of our proposed system compared with other methods. Finally, the conclusion is summarized in Section 6.

II. Scalp EEG Database

One of the databases utilized in this study is the CHB-MIT scalp EEG database [33], in which EEG recordings were collected from 23 pediatric subjects with intractable seizures at the Children's Hospital Boston. The sampling rate of all EEG recordings is 256 samples per second with a resolution of 16 bit [34]. The International 10-20 system of EEG electrode positions and nomenclature were used for these recordings [34]. There exist approximately 983 h of EEG recordings, including 198 identified seizures in this database. The starting and ending time of all seizures have been manually annotated by clinical experts after visual inspection. About 977 h of scalp EEG recordings containing 185 seizure events are adopted in this study. 31.6h of recordings, including 54 seizure events, are served as training set, while 945.3 h of EEG data with 131 seizures are deployed for testing the performance of our system. Generally, the SVM model with more training data could achieve a better generalization ability. To increase the amount of training data and reduce the possibility of overfitting, the length of non-seizure training data is selected as 4 times that of seizure signals and these seizure data are up-sampled 4 times using a sliding window with 0.5-s overlap. The information about seizure type, seizure onset zone, and other experimental details are summarized in Table I.

The other database used in this study was prepared by the Second Hospital of Shandong University (SH-SDU), Jinan, China. The SH-SDU database contains 198 h of scalp EEG recordings from 10 epilepsy patients with a sampling rate of 256 Hz. There are 191 seizures in this database and at least 3 seizures for each patient. For each seizure event, the duration, start time, and end time have been labeled explicitly according to expert judgments. Table II describes more details about each patient and the number of seizure events for training.

III. Method

The patient-specific seizure onset detection system proposed in this study consists of four stages, including pre-processing, CSP, classification with a SVM group, and post-processing. In the pre-processing stage, the scalp EEG segments are filtered and decomposed respectively by wavelet transformation and EMD, which could remove various artifacts from EEG signals automatically. The post-processing includes threshold decision, multi-SVM fusion, moving average filtering (MAF), and collar technique. Figure 1 describes the outline of the proposed system.

A. Wavelet Transform

In this work, EEG signals are firstly segmented into 2-s epochs (512 points) using a sliding window with no overlap in order to analyse EEG's non-stationary and transient characteristics better. Each epoch of EEG can be expressed as $d \in R^{M\times 512}$, where M is the number of channels. Then the EEG in each channel is decomposed with the six-level discrete wavelet transform (DWT) utilizing a db4 wavelet [4], [35]. Since the sample rate of EEG data is 256 Hz, coefficients D_1, D_2, D_3, D_4, D_5, D_6 and A_6 represent the components of original EEG within frequency band of 64-128 HZ, 32-64 HZ, 16-32 HZ, 8-16 HZ, 4-8 HZ, 2-4 HZ and 0-2 HZ, respectively. In general, the EEG of most seizures has frequencies between 2 and 29 Hz [36], [37]. Therefore, we only select four coefficients

TABLE I
DETAILS OF THE CHB-MIT DATABASE USED IN THIS STUDY

Patient	Gender	Age (years)	Seizure type	Seizure onset zone	Number of EEG channels	Number of seizures	Number of training seizures	Duration of recordings(h)
1	F	11	SP, CP	Temporal	23	7	1	40.55
2	M	11	SP, CP, GTC	Frontal	23	3	1	35.27
3	F	14	SP, CP	Temporal	23	7	1	38.00
4	M	22	SP, CP, GTC	Temporal, Occipital	23	4	2	156.07
5	F	7	CP, GTC	Frontal	23	5	1	39.00
6	F	1.5	CP, GTC	Temporal	23	10	4	66.74
7	F	14.5	SP, CP, GTC	Temporal	23	3	1	67.05
8	M	3.5	SP, CP, GTC	Temporal	23	5	1	20.00
9	F	10	CP, GTC	Frontal	23	4	2	67.87
10	M	3	SP, CP, GTC	Temporal	23	7	1	50.02
11	F	12	SP, CP, GTC	Frontal	23	3	1	34.79
12	F	2	SP, CP, GTC	Frontal	23	27	8	20.69
13	F	3	SP, CP, GTC	Temporal, Occipital	18	12	4	33.00
14	F	9	CP, GTC	Temporal	23	8	3	26.00
15	M	16	SP, CP, GTC	Frontal, Temporal	23	20	3	39.00
16	F	7	SP, CP, GTC	Temporal	18	10	6	19.00
17	F	12	SP, CP, GTC	Temporal	18	3	1	21.01
18	F	18	SP, CP	Temporal, Occipital	23	6	2	34.63
19	F	19	SP, CP, GTC	Frontal	23	3	1	28.93
20	F	6	SP, CP, GTC	Temporal	23	8	2	27.60
21	F	13	SP, CP	Temporal	23	4	1	32.83
22	F	9	-	Temporal, Occipital	23	3	1	31.00
23	F	6	-	Frontal	23	7	1	26.56
24	-	-	-	-	23	16	5	21.30
Total	-	-	-	-	-	185	54	976.93

Note: GTC = generalized tonic-clonic seizure, CP = complex partial seizures, SP = simple partial seizures.

TABLE II
DETAILS OF THE SH-SDU DATABASE USED IN THIS STUDY

Patient	Gender	Age (years)	Number of EEG channels	Number of seizures	Number of training seizures	Duration of recordings(h)
1	F	28	18	16	3	20.58
2	F	28	18	11	3	23.75
3	M	61	18	10	2	16.04
4	M	34	18	10	2	12.00
5	M	72	18	29	4	15.56
6	M	79	18	38	5	17.38
7	M	71	18	4	1	17.22
8	M	76	18	3	1	12.00
9	F	38	18	4	2	06.00
10	M	49	18	66	5	57.50
Total	-	-	-	191	28	198.03

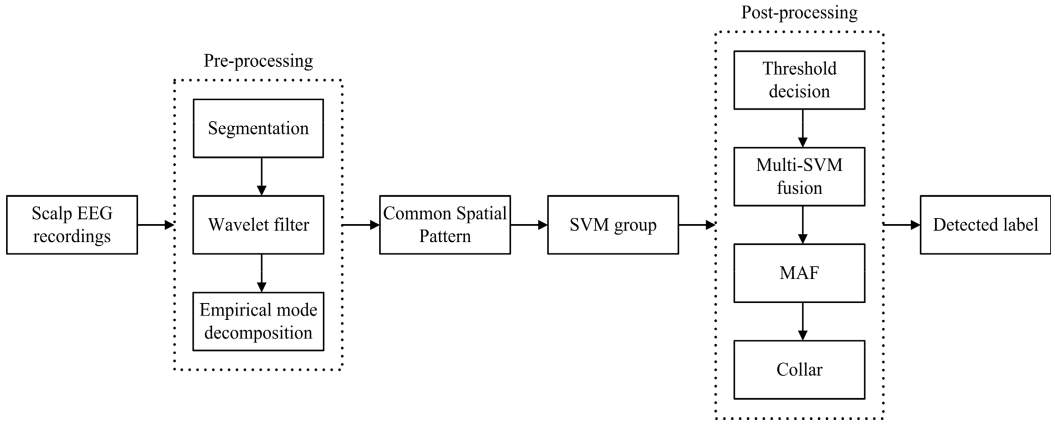

Fig. 1. The system diagram of the proposed method. The main steps contain pre-processing, CSP, SVM group and post-processing.

D_3, D_4, D_5 and D_6 to reconstruct signals S_3, S_4, S_5 and S_6. After that, the filtered signal $S = S_3 + S_4 + S_5 + S_6$ is obtained.

B. Empirical Mode Decomposition

Empirical Mode Decomposition (EMD) is an entirely data-driven algorithm that decomposes a nonstationary signal into multiple components termed Intrinsic Mode Functions (IMFs) [38]-[40]. For each IMF, two basic criteria should be satisfied: (1) in the entire time domain, the number difference between extreme points and zero crossings is zero or one [30]; (2) at every point, the mean value of the envelopes defined by the local maximum and local minimum amplitude is zero [30]. The algorithm can be performed as follows:

Given an input signal $s(t)$, $r(t) = s(t)$, $n = 1$.

Step 1: Identify the local maxima and local minima of $s(t)$.

Step 2: Connect the local minima and maxima using cubic spline functions, respectively, to determine a lower envelope $e_{lower}(t)$ and an upper envelope $e_{upper}(t)$.

Step 3: The mean value $m(t)$ is calculated from the average of two envelopes:

$$m(t) = \frac{e_{upper}(t) + e_{lower}(t)}{2} \tag{1}$$

Step 4: Get the resulting function $f(t)$ by subtracting the mean $m(t)$ from the input signal $s(t)$:

$$f(t) = s(t) - m(t) \tag{2}$$

Step 5: If $f(t)$ satisfies the criteria described above, an IMF component and the residual component $r(t)$ can be described as:

$$IMF_n = f(t) \tag{3}$$

$$r(t) = r(t) - f(t) \tag{4}$$

$$n = n + 1 \tag{5}$$

and then go to step 6. If not, $s(t) = f(t)$ and go back to step 1.

Step 6: The decomposition is stopped when the residual component $r(t)$ obtained from (5) is a monotonic function, otherwise, $s(t) = r(t)$ and go back to step 1.

According to the algorithm described above, a segment of EEG signal is separated into N IMFs and a residual component $r(t)$:

$$s(t) = \sum_{n=1}^{N} f_n(t) + r(t) \tag{6}$$

An epoch of scalp EEG from Patient 22 and its five IMFs are shown in Figure 2. The data between 0 and 5 seconds belong to inter-ictal EEG signals, and the data of 5-10 seconds are epileptic seizure signals. As can be seen in Figure 2, the difference between ictal and inter-ictal scalp EEG is mainly related to IMF2. Therefore, we extract IMF2 of each segment of EEG to represent the overall signal. For a 2-s EEG epoch, the output of EMD processing is a $M \times 512$ matrix. After that, we further divide the matrix into 4 segments of 0.5s (128 points) without overlap, and feed each $M \times 128$ matrix into the following CSP algorithm.

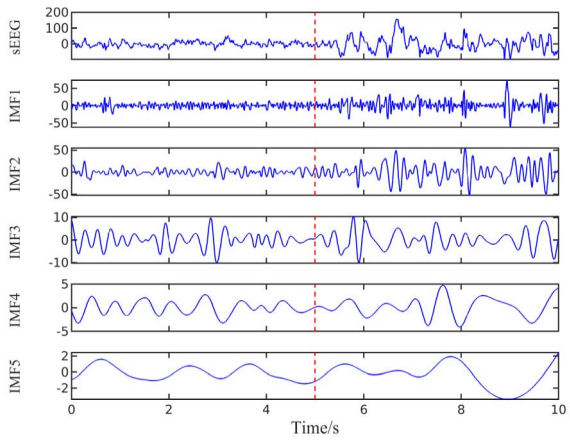

Fig. 2. An epoch of scalp EEG from Patient 22 in the CHB-MIT database and its five IMFs.

C. Common Spatial Pattern

CSP is a statistical method that constructs a projection matrix W to project multi-channel EEG segments into a low-dimensional space, so that the variance of one class is maximized and the other is minimized [28], [41]. The matrix W can be calculated as follows.

Step 1: The normalized spatial covariance C of the EEG segment $D \in R^{M \times L}$ can be defined as:

$$C = \frac{DD^T}{trace\left(DD^T\right)} \tag{7}$$

where M is the number of EEG channels, L is the number of samples, and T represents the transpose operation.

Step 2: Get two discriminated spatial covariance C_1 (inter-ictal state) and C_2 (ictal state) by averaging over the spatial covariance of each class ($i = 1, 2$), and compose a covariance matrix C_c by

$$C_c = C_1 + C_2 \tag{8}$$

Step 3: Calculate the diagonal matrix Σ of eigenvalues and the corresponding eigenvector matrix F_c by decomposing the covariance matrix C_c:

$$C_c = F_c \Sigma F_c^T \tag{9}$$

Step 4: Obtain a matrix P utilizing whitening transformation:

$$P = \sqrt{\Sigma^{-1}} F_c^T \tag{10}$$

and then two matrices S_1 and S_2 can be given as:

$$S_1 = PC_1P^T = U\Lambda_1U^T \tag{11}$$

$$S_2 = PC_2P^T = U\Lambda_2U^T \tag{12}$$

where S_1 and S_2 share the same eigenvectors. $\Lambda_1 + \Lambda_2 = I$, where I is the identity matrix. The eigenvalues are then sorted in descending order. Thus the CSP projection matrix W_0 is formulated as:

$$W_0 = U^T P \in R^{M \times M} \tag{13}$$

In this study, the first m and the last m rows of matrix W_0 are extracted to construct a new spatial filter $W(W \in R^{2m\times M}, 1 \leq m \leq M/2, m \in Z)$ which aims to enhance features and reduce dimensionality of original data. The filtered data D_f by CSP is calculated for the segment $D \in R^{M\times L}$:

$$D_f = WD \in R^{2m\times L} \tag{14}$$

Finally, the variance of each row in matrix D_f is calculated to obtain a $2m \times 1$ matrix Var, which is used as the only feature of the EEG segment $D \in R^{M\times L}$. In our work, 10 spatial filters are trained for each patient. The inputs of each CSP include ictal data $D_{Ictal} \in R^{M\times L\times K}$ (K is the number of segments), inter-ictal data $D_{Inter_i} \in R^{M\times L\times K}$ ($i \in [1, 10]$) and $m(m = 4)$. We will use the 10 trained spatial filters to extract variance of testing data and feed them into 10 SVMs for classification, respectively.

D. Support Vector Machine Group

SVM is a popular machine learning algorithm which can designs a hyperplane (decision boundary) in feature space to realize a binary classification [42], [43]. The simplest case is a linear SVM for linearly separable data [43]. The linear kernel function is defined as:

$$K\left(x_i, x_j\right) = x_i^T x_j \tag{15}$$

In the case of non-linear classification, the main idea of SVM is applying other kernel functions to map original signals into a new higher dimensional feature space where a hyperplane separating different classes may exist [43]. Commonly there are two kinds of kernel functions widely used. The first type is the radial basis function (RBF), which can be expressed as:

$$K\left(x_i, x_j\right) = \exp\left(-\frac{\left\|x_i - x_j\right\|^2}{2\sigma^2}\right) \tag{16}$$

where σ ($\sigma > 0$) is the bandwidth of Gaussian kernel. The other is the polynomial kernel function with the equation below:

$$K\left(x_i, x_j\right) = \left(x_i^T x_j\right)^d \tag{17}$$

where d ($d \geq 1$) is the number of polynomials. Note that if d is equal to 1, the polynomial kernel function is actually a linear kernel function. The d used in our study is 3 and the function is defined as a cubic kernel function.

In this study, SVM is chosen as the classifier to solve the problems that original EEG features are linearly inseparable and small samples of training data. Furthermore, a SVM group consisting of 10 SVMs is constructed based on the idea of ensemble learning. For each patient, we employed the same seizure data and different non-seizure data to train different SVM in the SVM group. Moreover, we use 5-fold cross-validation in training set to select the kernel expression with optimal sensitivity and accuracy among linear, gauss and polynomial functions, and utilize the selected function as the kernel function of SVMs for testing. The output of a single SVM is the score DL_{1i} ($i \in [1, 10]$) corresponding to 0.5-s epochs (128 points) of EEG recordings. We define the score DL_{2i} ($i \in [1, 10]$), which corresponds to 2-s epochs, as the sum of four points in DL_{1i} ($i \in [1, 10]$). The 2-s epoch with the higher score has a greater chance to belong to a seizure.

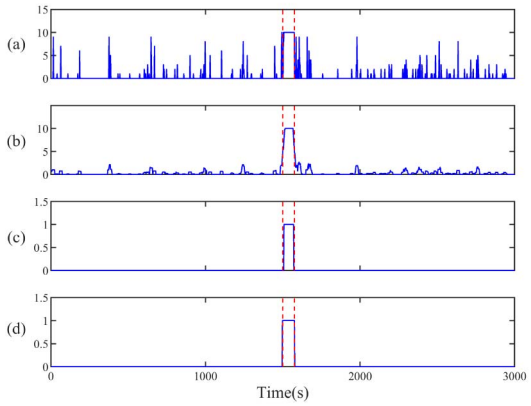

Fig. 3. The post-processing procedure of 3000-s scalp EEG data. (a) The integrated score from the SVM group. (b) The score after smoothing. (c) The binary value after threshold decision. (d) The detected result after 'collar' operation.

E. Post-Processing

Threshold decision, multi-SVM fusion, moving average filter, and collar operation are employed to the output score of the above SVM group for improving detection results. Figure 3 illustrates the post-processing procedure of 3000-s scalp EEG. The score DL_{2i} ($i \in [1, 10]$) is firstly compared with a threshold $T1$ to acquire 10 binary decisions DL_{3i} ($i \in [1, 10]$) where 0 represents non-seizure segment and 1 for seizure segment. We define the integrated score (Figure 3a), ranging from 0 to 10, as the sum of 10 binary decisions DL_{3i} ($i \in [1, 10]$). And then the moving average filter (MAF) is applied to this integrated score to reduce false detection rate and limit the impact of artifacts (Figure 3b). The MAF filter is described as:

$$Z(i) = \frac{1}{2M+1}\sum_{k=-M}^{M} x(i+k) \tag{18}$$

where x is the integrated score, Z is the filtered score, $2M+1$ denotes the length of smoothing which is specific for each patient. The label DL_4 (Figure 3c) is obtained by comparing the filtered score with a threshold $T2$ in the interval [0 10]. Owing to the fact that the MAF may cut off the onset and ending of seizure events, a collar operation is applied to compensate for the missing parts of a seizure [44], that is, each seizure decision in the label DL_4 is extended T_{collar} points at either side (Figure 3d) to compensate for the points discarded by MAF. For each patient, the training dataset is employed to obtain the value of $T1$, $T2$, M, and T_{collar}, and then these parameters are adapted to achieve an optimal accuracy.

F. Identification of Seizure Onset Channels

The CSP serves as a feature extractor in above seizure detection process, which can reduce the computational complexity

and enhance characteristics of variance. Meanwhile, CSP is also helpful to analyze which EEG channels are related to seizure onsets. For each patient, the first 4-s EEG from each seizure event are extracted, and 4-s data are segmented into 2-s epochs using a sliding window with 0.5-s overlap, which obtains $Focus_{ictal} \in R^{23^*512^*5}$. Furthermore, for each seizure event, we randomly select 50-s inter-ictal data in the first 1-h EEG recordings, and they are segmented into 2-s epochs with no overlap, which obtains $Focus_{Inter} \in R^{23^*512^*25}$. Each obtained 2-s epoch is filtered with WT and EMD, respectively. Then we feed the filtered EEG into the CSP algorithm to train 5 spatial filters SF_p $(p \in [1, 5])$. The weight matrix W_p is acquired by taking absolute values for each element in the transposed matrix of each SF_p:

$$W_p = \left| SF_p^T \right| \tag{19}$$

where each W_p is a $23 \times 2m$, $(m = 4)$ positive real matrix. Afterwards, we obtain the mean weight matrix W_{mean} from averaging 5 W_p, and sum all elements of each row in W_{mean} to get S_w:

$$W_{mean} = \frac{1}{5} \sum_{p=1}^{5} W_p \tag{20}$$

$$S_{w_{i1}} = \sum_{j=1}^{2m} W_{mean_{ij}} \tag{21}$$

where the nth value in S_w indicates contributions of the data from nth channel to characterize epilepsy. The channel with the larger value could characterize the differences between seizure and non-seizure data better. We arrange values of S_w in descending order, and select 3 channels corresponding to the first 3 maximum values as EEG channels involved in seizure onsets.

IV. Results

All experiments were carried out in MATLAB software with version of 9.5.0 (R2018b), running in a workstation with an Intel E5-2667v4 CPU and 64GB memory. Two criteria, the segment-based criterion and the event-based criterion, were employed to evaluate the performance of the proposed detection method.

At the segment-based level, the system performance is assessed in terms of three parameters including sensitivity, specificity and accuracy:

$$Sensitivity = \frac{TP}{TP + FN} \times 100\% \tag{22}$$

$$Specificity = \frac{TN}{TN + FP} \times 100\% \tag{23}$$

$$Accuracy = \frac{TP + TN}{TP + FN + TN + FP} \times 100\% \tag{24}$$

where TP, TN, FP and FN represent true positive, true negative, false positive and false negative, respectively.

Event-based criterion is an effective tool to measure the system feasibility in clinical applications as well. The criterion contains sensitivity and false detection rate (FDR). If the seizure segment detected by our proposed method is also marked by the epilepsy expert, it is viewed as a true detected seizure event, and if not, it is confirmed as a false judgment. For each patient, sensitivity is the ratio of the number of true detected seizure events to that labeled by experts, and FDR is the mean number of times in an hour that the inter-ictal data is wrongly detected as the seizure event.

TABLE III
CHB-MIT Detection Results of the Proposed Method at the Segment-Based Level

Patient	Sensitivity (%)	Specificity (%)	Accuracy (%)
1	100	99.09	99.09
2	100	99.72	99.72
3	100	98.13	98.14
4	90.85	92.94	92.93
5	100	99.73	99.73
6	100	98.38	98.38
7	92.62	90.26	90.26
8	94.68	93.16	93.17
9	100	99.63	99.64
10	100	99.53	99.53
11	98.01	99.97	99.96
12	87.80	95.36	95.28
13	82.74	94.36	94.32
14	96.92	98.53	98.53
15	99.17	99.14	99.14
16	100	90.18	90.19
17	100	98.84	98.84
18	97.56	98.15	98.15
19	100	99.44	99.44
20	99.01	97.59	97.59
21	100	99.79	99.79
22	100	99.82	99.82
23	100	98.84	98.84
24	100	99.35	99.35
Average	97.34	97.50	97.49

A. Results From the CHB-MIT Database

The detection results at the segment-based level are described in Table III. In average for all patients, the system achieved a mean sensitivity of 97.34% and a mean specificity of 97.50%. A total of 13 subjects have the sensitivity of 100% on the basis of ensuring specificity higher than 98%. Furthermore, excepting for 5 subjects (Patient 4, 7, 8, 12 and 13), all subjects have specificity and recognition accuracy of more than 97%. The best result, the sensitivity of 100% with the specificity of 99.82%, is acquired from patient 22. However, there also exists an unsatisfactory result that patient 13 has the lowest sensitivity which is only 82.74%. According to his EEG recordings, we find that the brain electrode connection was changed 5 times, which may introduce noise into signals and affect the detection results.

In terms of the event-based performance evaluation, there were 131 seizures employed to assess the proposed seizure detection system and a total of 129 seizures were detected successfully. All of the subjects, excepting for Patient 12, have no undetected seizure events. The average sensitivity and average FDR of our system are 98.47% and 0.63/h, respectively. It is worth mentioning that the false detection rates of 11 subjects are less than 0.2/h, despite the impact of

TABLE IV
CHB-MIT DETECTION RESULTS OF THE PROPOSED METHOD AT THE EVENT-BASED LEVEL

Patient	Number of marked seizures	Number of true detections	Sensitivity (%)	FDR (/h)
1	6	6	100	0.10
2	2	2	100	0.23
3	6	6	100	0.26
4	2	2	100	0.06
5	4	4	100	0.03
6	6	6	100	0.57
7	2	2	100	0.72
8	4	4	100	0.25
9	2	2	100	0.03
10	6	6	100	0.04
11	2	2	100	0
12	19	17	89..47	2.85
13	8	8	100	4.25
14	5	5	100	0.54
15	17	17	100	0.20
16	4	4	100	3.76
17	2	2	100	0.05
18	4	4	100	0.24
19	2	2	100	0.17
20	6	6	100	0.37
21	3	3	100	0.03
22	2	2	100	0
23	6	6	100	0.12
24	11	11	100	0.30
Total	131	129	98.47	0.63

Note: FDR = false detection rate

much noise in scalp EEGs. The performance of the proposed method based on the event-based criterion is provided in Table IV.

B. Results From the SH-SDU Database

Similar to CHB-MIT database, recordings from the SH-SDU database are 18-channel scalp EEG data. However, there might be more artefacts in EEGs according to the clinical manifestations of patients described by local doctors. Table V shows the detection results of all 10 patients at the segment-based performance evaluation. The mean sensitivity, mean specificity and mean recognition are 93.67%, 96.06% and 95.99%, respectively. The highest sensitivity of 100% with the specificity of 99.97% is obtained from Patient 9. All patients have the specificity of more than 91%, and there exist only 2 patients having the sensitivity below 90%.

For the event-based evaluation, the seizure detection method described here yielded a mean sensitivity of 99.39% and a mean FDR of 0.64/h. We used 163 seizures totally in this work, and 162 seizure events were detected correctly by the proposed system. More detailed results for SH-SDU database with the event-based criterion are listed in Table VI.

C. The Predicted Channels Involved in Seizure Onsets

The EEG electrodes in CHB-MIT database are bipolar channels which represent the difference between EEG recordings of two brain positions. We hope that, with the help of CSP spatial filters, relevant scalp electrodes related to the seizure onset could be found, and corresponding brain regions could be determined using bipolar channels.

Figure 4 presents a detection result for the focal channels of Patient 1 in CHB-MIT database, which are marked using red

TABLE V
SH-SDU DETECTION RESULTS OF THE PROPOSED METHOD AT THE SEGMENT-BASED LEVEL

Patient	Sensitivity (%)	Specificity (%)	Accuracy (%)
1	94.05	98.28	98.25
2	90.00	96.20	96.16
3	85.62	97.81	97.29
4	100	99.60	99.61
5	92.46	95.04	94.85
6	95.86	91.48	91.68
7	95.93	92.16	92.45
8	100	95.79	95.82
9	100	99.97	99.97
10	82.76	94.26	93.82
Average	93.67	96.06	95.99

TABLE VI
SH-SDU DETECTION RESULTS OF THE PROPOSED METHOD AT THE EVENT-BASED LEVEL

Patient	Number of marked seizures	Number of true detections	Sensitivity (%)	FDR (/h)
1	13	13	100	0.55
2	8	8	100	0.45
3	8	8	100	0.08
4	8	8	100	0.18
5	25	25	100	0.82
6	33	33	100	2.13
7	3	3	100	0.73
8	2	2	100	0
9	2	2	100	0
10	61	60	98.36	1.48
Total	163	162	99.39	0.64

Note: FDR = false detection rate

circles. All marked channels in Fig.4 are related to both sides of the temporal lobe, so we believe that the seizure onset area of Patient 1 is closest to temporal regions. We predicted the most probable brain region(s) related to seizure onset for each patient in CHB-MIT database. Table VII shows the predicted EEG channels involved in seizure onsets and the comparison between predicted and reference areas. We found that, for most patients of CHB-MIT database, the channel with the larger CSP weight has more obvious epileptic characteristics at the beginning of a seizure. As shown in Table VII, except for Patient 2, 16, 17 and 19, the predicted regions of 19 out of 23 patients are close to reference. These results show that, without other auxiliary instruments, CSP is helpful to analyse which EEG channels are involved in the seizure onset.

V. DISCUSSION

A novel seizure onset detection algorithm based on EMD and CSP is provided in this paper. To observe which frequency components obtained by EMD can distinguish ictal data from inter-ictal data best, IMF1, IMF2, IMF3, and the sum of IMF1 and IMF2 are used to represent signals respectively for epilepsy detection. We randomly selected 20 patients (CHB-MIT: 14 patients, SH-SDU: 6 patients) for assessment, and the detection results including the sensitivity and specificity are shown in Figure 5. As can be seen, the sensitivity and specificity with IMF2 are best. Therefore, the IMF2 of EEG segments are selected for feature extraction.

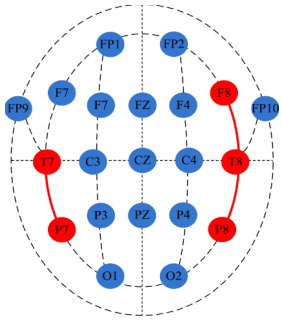

Fig. 4. The channels involved in seizure onset are predicted by our method. The red circles represent the seizure onset electrodes, and red lines are their bipolar connections.

TABLE VII
THE PREDICTED EEG CHANNELS INVOLVED IN SEIZURE ONSET AND THE COMPARISON BETWEEN PREDICTED AND REFERENCE AREAS

Patient	Reference area	Predicted area	Main channels (Top three)
1	T	T	T8-P8, T7-P7, F8-T8
2	F	T-O	T7-P7, P8-O2, T8-P8
3	T	T, F	T8-P8, F7-T7, FP2-F8
4	T, O	T-O	T8-P8, T7-P7, P4-O2
5	F	T, F	T7-P7, T8-P8, FT9-FT10
6	T	T	T8-P8, FT10-T8, T7-P7
7	T	T-O	T7-P7, T8-P8, P7-O1
8	T	T	T7-P7, T8-P8, FT10-T8
9	F	T, F	T8-P8, FT10-T8, FP2-F8
10	T	T	T8-P8, T7-P7, T7-FT9
11	F	T, F	T7-P7, F3-C3, F4-C4
12	F	T, F	T8-P8, FP1- F7, FP2-F8
13	T, O	P, O	P4-O2, C3-P3, C4-P4
14	T	T, P	T7-P7, T8-P8, P3-O1
15	F, T	F T	FT10-T8, T8-P8, T7-P7,
16	T	F, P	FP2-F4, P8-O2, P4-O2
17	T	F, P	F3-C3, P3-O1, F4-C4
18	T, O	T-O	T7-P7, T8-P8, P7-O1
19	F	T	T8-P8, T7-P7, C3-P3
20	T	T, F	T8-P8, T7-P7, FP2-F4
21	T	T	T7-P7, T8-P8, T7-FT9
22	T, O	T	T8-P8, T7-P7, FT10-T8
23	F	T, F	T8-P8, FT10-T8, FP2-F4
24	-	T	T7-P7, T8-P8, FT10-T8

Note: T = Temporal, F = Frontal, O = Occipital, P = Parietal, T-O = Temporal - Occipital - Parietal

In order to study the importance of EMD, we present a comparison between classification performance with and without EMD. The system without EMD was validated on the CHB-MIT database, where it achieved an average sensitivity of 88.44% with an average specificity of 95.45%. Since the difference in specificity between two methods was small, the segment-based sensitivity from each patient is compared in Figure 6. In the absence of EMD, only 8 patients have the same sensitivity as before, and it is worth mentioning that the sensitivity of 11 patients are significantly lower than the results with EMD. In addition, we also calculated the time consumed in using EMD to decompose 4-s EEG data. It took about 0.0167 seconds to decompose a 4-s, 23-channel EEG with EMD, and only about 35.098 seconds to detect 1-h, 23-channel EEG recordings totally, which could meet the needs of real-time detection. Hence, it can be seen that EMD plays a prominent role in the proposed system.

As shown in Reference area of Table VII, 19 out of 23 seizure onset regions are related to temporal or frontal.

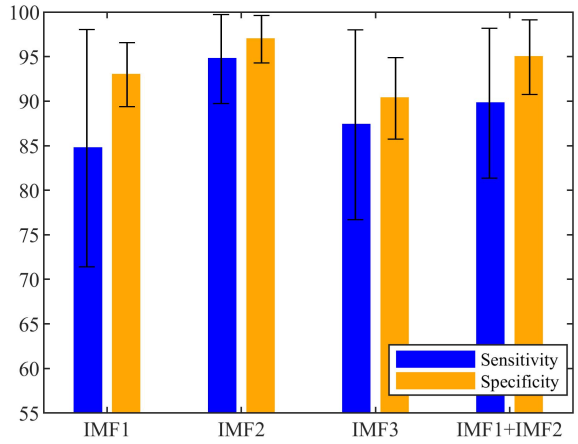

Fig. 5. The result comparison of four IMF components.

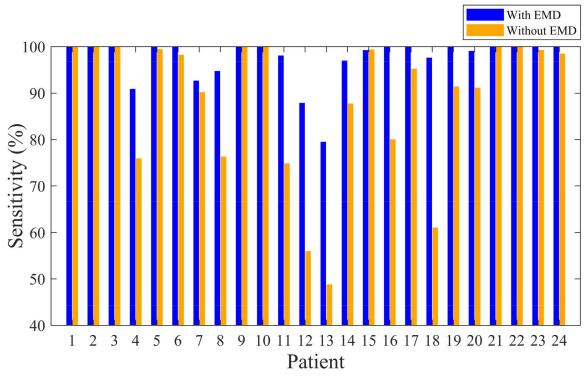

Fig. 6. The comparison between results with EMD and without EMD.

To evaluate the effects of CSP, we manually selected 8 electrodes closer to both sides of frontal and temporal regions such as Channel FP1-F7, F7-T7, T7-P7, T7-FT9, FP2-F8, F8-T8, T8-P8 and FT10-T8, to detect seizures for 24 subjects. The experimental results showed that only 5 subjects (Patient 2, 3, 9, 22 and 24) had the same sensitivity as before, and the remaining results were much lower. Compared with the results using CSP, the mean sensitivity without CSP was reduced by about 8% based on similar specificity. These comparisons revealed that the utilization of CSP could improve the overall performance for seizure onset detection.

The CHB-MIT scalp EEG database has been employed to evaluate the performance of many other seizure detection approaches. Zabihi *et al.* [45] proposed a system combining nonlinear dynamics with Linear Discriminant Analysis (LDA) and Artificial Neural Network (ANN), which introduced the nullcines concept to extract discriminative features and yielded a mean sensitivity of 91.15% with mean specificity of 95.16%. Yuan *et al.* [46] presented a detector, which was assessed on 958.2 h of EEG data from 24 patients, using the earth mover's distance and BLDA classifier. An average specificity of 95.75% and sensitivity of 95.65% were achieved. In the work of Tsiouris *et al.* [47], an unsupervised system for seizure detection was developed. Their method was tested on 980 h of EEG recordings from 24 epileptic patients in the same database, which obtained a specificity of 95%, a sensitivity of 89%, and a false positive rate of 8.1/h. Compared with these approaches, our proposed method achieved the

TABLE VIII
COMPARISON OF THE PERFORMANCE FOR DIFFERENT METHODS ON CHB-MIT DATASET

Method	Total of EEG data(h)	Av. Sen. (%)	Av. Spec. (%)	Event Sen. (%)	FDR(/h)
Zabihi et al[45]	172	91.15	95.16	—	—
Yuan et al[46]	958.2	95.65	95.75	94.48	0.68
Tsiouris et al[47]	980	—	95.00	89.00	8.10
Selvakumari et al[48]	—	97.50	94.50	—	—
Bhattacharyya et al[49]	178	97.91	99.57	—	—
This work	976.9	97.34	97.50	98.47	0.63

higher sensitivity and specificity. Selvakumari *et al.* [48] presented a patient-specific seizure onset detection system utilizing Hybrid Classifier with optimized electrodes. In their study, 23 channels were divided into 4 different kinds of combinations according to the location of electrodes and the particular function of the brain. The best sensitivity of 97.5% and specificity of 94.5% were obtained with the electrodes responsible for vision and hearing. In comparison to their system, the specificity of our system is obviously improved, although the sensitivity is slightly lower. Additionally, the provided methodology in this paper is more concise and does not need to manually set the combination of channels. Bhattacharyya and Pachori [49] proposed a multivariate approach based on empirical wavelet transform. For each patient, they applied mutual information with the least standard deviation to select the best 5 channels to represent overall data. This approach obtained the mean sensitivity of 97.91% and the mean specificity of 99.57% using 178 h of EEGs. Despite the wonderful performance, they did not make a comprehensive study of the database. Moreover, our presented system can reduce the dimensions of EEGs automatically, the computational burden of which is less than that of mutual information. Table VIII shows a comparison between the results of our method and other methods for seizure detection in recent years.

VI. CONCLUSION

In this paper, we proposed a novel patient-specific seizure onset detection system based on EMD and CSP. The EMD is used on the filtered EEG to further improve the SNR, and CSP compresses the dimensionality of signals for reducing the computational burden and extracts the variance as a unique feature. The system was evaluated on scalp EEG recordings from 34 subjects of two databases. The experimental results indicated that our proposed algorithm achieved a sensitivity of 97.34% with a specificity of 97.50% in CHB-MIT database and a sensitivity of 93.67% with a specificity of 96.06% in SH-SDU database. Moreover, the CSP spatial filter was served as a multi-channel weight matrix and utilized to identify EEG channels involved in seizure onsets automatically. For 23 subjects, the seizure onset areas of 19 patients were correctly predicted. To sum up, these satisfactory results may provide a reference for epilepsy diagnosis in clinical applications.

REFERENCES

[1] H. Witte, L. D. Iasemidis, and B. Litt, "Special issue on epileptic seizure prediction," *IEEE Trans. Biomed. Eng.*, vol. 50, no. 5, pp. 537–539, May 2003.

[2] H. Adeli, Z. Zhou, and N. Dadmehr, "Analysis of EEG records in an epileptic patient using wavelet transform," *J. Neurosci. Methods*, vol. 123, no. 1, pp. 69–87, Feb. 2003.

[3] S. Grewal and J. Gotman, "An automatic warning system for epileptic seizures recorded on intracerebral EEGs," *Clin. Neurophysiol.*, vol. 116, no. 10, pp. 2460–2472, Oct. 2005.

[4] X. Ma, N. Yu, and W. Zhou, "Using dictionary pair learning for seizure detection," *Int. J. Neural Syst.*, vol. 29, no. 04, May 2019, Art. no. 1850005.

[5] R. Agarwal, J. Gotman, D. Flanagan, and B. Rosenblatt, "Automatic EEG analysis during long-term monitoring in the ICU," *Electroencephalogr. Clin. Neurophysiol.*, vol. 107, no. 1, pp. 44–58, Jul. 1998.

[6] H. Qu and J. Gotman, "Improvement in seizure detection performance by automatic adaptation to the EEG of each patient," *Electroencephalogr. Clin. Neurophysiol.*, vol. 86, no. 2, pp. 79–87, Feb. 1993.

[7] Y. U. Khan and J. Gotman, "Wavelet based automatic seizure detection in intracerebral electroencephalogram," *Clin. Neurophysiol.*, vol. 114, no. 5, pp. 898–908, May 2003.

[8] R. Hussein, H. Palangi, R. K. Ward, and Z. J. Wang, "Optimized deep neural network architecture for robust detection of epileptic seizures using EEG signals," *Clin. Neurophysiol.*, vol. 130, no. 1, pp. 25–37, Jan. 2019.

[9] P. LeVan, E. Urrestarazu, and J. Gotman, "A system for automatic artifact removal in ictal scalp EEG based on independent component analysis and Bayesian classification," *Clin. Neurophysiol.*, vol. 117, no. 4, pp. 912–927, Apr. 2006.

[10] J. Gotman, "Automatic recognition of epileptic seizures in the EEG," *Electroencephalogr. Clin. Neurophysiol.*, vol. 54, no. 5, pp. 530–540, 1982.

[11] G. R. Minasyan, J. B. Chatten, M. J. Chatten, and R. N. Harner, "Patient-specific early seizure detection from scalp electroencephalogram," *J. Clin. Neurophysiol.*, vol. 27, no. 3, pp. 163–178, Jun. 2010.

[12] T. Zhang and W. Chen, "LMD based features for the automatic seizure detection of EEG signals using SVM," *IEEE Trans. Neural Syst. Rehabil. Eng.*, vol. 25, no. 8, pp. 1100–1108, Aug. 2017.

[13] F. Riaz, A. Hassan, S. Rehman, I. K. Niazi, and K. Dremstrup, "EMD-based temporal and spectral features for the classification of EEG signals using supervised learning," *IEEE Trans. Neural Syst. Rehabil. Eng.*, vol. 24, no. 1, pp. 28–35, Jan. 2016.

[14] A. Bhattacharyya, V. Gupta, and R. B. Pachori, "Automated identification of epileptic seizure EEG signals using empirical wavelet transform based Hilbert marginal spectrum," in *Proc. 22nd Int. Conf. Digit. Signal Process. (DSP)*, Aug. 2017, pp. 1–5.

[15] Y. Kumar, M. L. Dewal, and R. S. Anand, "Epileptic seizure detection using DWT based fuzzy approximate entropy and support vector machine," *Neurocomputing*, vol. 133, pp. 271–279, Jun. 2014.

[16] A. Bhattacharyya, R. Pachori, A. Upadhyay, and U. Acharya, "Tunable-Q wavelet transform based multiscale entropy measure for automated classification of epileptic EEG signals," *Appl. Sci.*, vol. 7, no. 4, p. 385, Apr. 2017.

[17] R. Zarei, J. He, S. Siuly, G. Huang, and Y. Zhang, "Exploring douglas-peucker algorithm in the detection of epileptic seizure from multicategory EEG signals," *BioMed Res. Int.*, vol. 2019, Jul. 2019, Art. no. 5173589.

[18] H. R. Al Ghayab, Y. Li, S. Siuly, and S. Abdulla, "A feature extraction technique based on tunable Q-factor wavelet transform for brain signal classification," *J. Neurosci. Methods*, vol. 312, pp. 43–52, Jan. 2019.

[19] H. R. Al Ghayab, Y. Li, S. Siuly, and S. Abdulla, "Epileptic seizures detection in EEGs blending frequency domain with information gain technique," *Soft Comput.*, vol. 23, no. 1, pp. 227–239, Jan. 2019.

[20] E. E. Swartzla, "Introduction to statistical pattern recognition—FUKUNAGA,K," *IEEE Trans. Syst. Man Cybern.*, vol. MC-4, no. 2, p. 238, Feb. 1974.
[21] Z. J. Koles, J. C. Lind, and P. Florhenry, "Spatial patterns in the background eeg underlying mental disease in man," *Electroencephalogr. Clin. Neurophysiol.*, vol. 91, no. 5, pp. 319–328, Nov. 1994.
[22] Y. Zhang, Y. Wang, J. Jin, and X. Y. Wang, "Sparse Bayesian learning for obtaining sparsity of eeg frequency bands based feature vectors in motor imagery classification," *Int. J. Neural Syst.*, vol. 27, no. 2, Mar. 2017, Art. no. 1650032.
[23] J. M. Hahne, B. Graimann, and K.-R. Muller, "Spatial filtering for robust myoelectric control," *IEEE Trans. Biomed. Eng.*, vol. 59, no. 5, pp. 1436–1443, May 2012.
[24] F. Riillo *et al.*, "Optimization of EMG-based hand gesture recognition: Supervised vs. Unsupervised data preprocessing on healthy subjects and transradial amputees," *Biomed. Signal Process. Control*, vol. 14, pp. 117–125, Nov. 2014.
[25] A. Rayatnia and R. Khanbabaie, "Common spatial patterns feature extraction and support vector machine classification for motor imagery with the secondbrain," *Int. J. Eng.*, vol. 32, no. 9, pp. 1284–1289, Sep. 2019.
[26] Y. Zhang, G. Zhou, J. Jin, Q. Zhao, X. Wang, and A. Cichocki, "Aggregation of sparse linear discriminant analyses for event-related potential classification in brain-computer interface," *Int. J. Neural Syst.*, vol. 24, no. 01, Feb. 2014, Art. no. 1450003.
[27] S. Khanmohammadi and C.-A. Chou, "Adaptive seizure onset detection framework using a hybrid PCA–CSP approach," *IEEE J. Biomed. Health Informat.*, vol. 22, no. 1, pp. 154–160, Jan. 2018.
[28] T. N. Alotaiby, S. A. Alshebeili, F. M. Alotaibi, and S. R. Alrshoud, "Epileptic seizure prediction using CSP and LDA for scalp EEG signals," *Comput. Intell. Neurosci.*, vol. 2017, Oct. 2017, Art. no. 1240323.
[29] N. E. Huang *et al.*, "The empirical mode decomposition and the Hilbert spectrum for nonlinear and non-stationary time series analysis," *Proc. Roy. Soc. London. Ser. A, Math., Phys. Eng. Sci.*, vol. 454, no. 1971, pp. 903–995, Mar. 1998.
[30] V. Bajaj and R. B. Pachori, "Classification of seizure and nonseizure EEG signals using empirical mode decomposition," *IEEE Trans. Inf. Technol. Biomed.*, vol. 16, no. 6, pp. 1135–1142, Nov. 2012.
[31] R. J. Martis *et al.*, "Application of empirical mode decomposition (EMD) for automated detection of epilepsy using eeg signals," *Int. J. Neural Syst.*, vol. 22, no. 6, Dec. 2012, Art. no. 1250027.
[32] S. Li, W. Zhou, Q. Yuan, S. Geng, and D. Cai, "Feature extraction and recognition of ictal EEG using EMD and SVM," *Comput. Biol. Med.*, vol. 43, no. 7, pp. 807–816, Aug. 2013.
[33] A. L. Goldberger *et al.*, "PhysioBank, PhysioToolkit, and PhysioNet: Components of a new research resource for complex physiologic signals," *Circulation*, vol. 101, no. 23, p. E30, Jun. 2000.
[34] J.-L. Song and R. Zhang, "Application of extreme learning machine to epileptic seizure detection based on lagged Poincare plots," *Multidimensional Syst. Signal Process.*, vol. 28, no. 3, pp. 945–959, Jul. 2017.
[35] Q. Yuan, W. Zhou, S. Li, and D. Cai, "Epileptic EEG classification based on extreme learning machine and nonlinear features," *Epilepsy Res.*, vol. 96, nos. 1–2, pp. 29–38, Sep. 2011.
[36] M. E. Saab and J. Gotman, "A system to detect the onset of epileptic seizures in scalp EEG," *Clin. Neurophysiol.*, vol. 116, no. 2, pp. 427–442, Feb. 2005.
[37] X. Liu *et al.*, "Clinical implications of scalp ictal EEG pattern in patients with temporal lobe epilepsy," *Clin. Neurophysiol.*, vol. 130, no. 9, pp. 1604–1610, Sep. 2019.
[38] P. Stepien, W. Klonowski, and N. Suvorov, "Nonlinear analysis of EEG in chess players," *EPJ Nonlinear Biomed. Phys.*, vol. 3, no. 1, pp. 1–9, Mar. 2015.
[39] E. Alickovic, J. Kevric, and A. Subasi, "Performance evaluation of empirical mode decomposition, discrete wavelet transform, and wavelet packed decomposition for automated epileptic seizure detection and prediction," *Biomed. Signal Process. Control*, vol. 39, pp. 94–102, Jan. 2018.
[40] C. M. Sweeney-Reed, S. J. Nasuto, M. F. Vieira, and A. O. Andrade, "Empirical mode decomposition and its extensions applied to EEG analysis: A review," *Adv. Data Sci. Adapt. Anal.*, vol. 10, no. 2, Apr. 2018, Art. no. 1840001.
[41] G. Huang, G. Liu, J. Meng, D. Zhang, and X. Zhu, "Model based generalization analysis of common spatial pattern in brain computer interfaces," *Cognit. Neurodyn.*, vol. 4, no. 3, pp. 217–223, Sep. 2010.
[42] R. Sharma, R. Pachori, and U. Acharya, "Application of entropy measures on intrinsic mode functions for the automated identification of focal electroencephalogram signals," *Entropy*, vol. 17, no. 2, pp. 669–691, Feb. 2015.
[43] N. Nicolaou and J. Georgiou, "Detection of epileptic electroencephalogram based on permutation entropy and support vector machines," *Expert Syst. Appl.*, vol. 39, no. 1, pp. 202–209, Jan. 2012.
[44] A. Temko, E. Thomas, W. Marnane, G. Lightbody, and G. Boylan, "EEG-based neonatal seizure detection with support vector machines," *Clin. Neurophysiol.*, vol. 122, no. 3, pp. 464–473, Mar. 2011.
[45] M. Zabihi, S. Kiranyaz, V. Jantti, T. Lipping, and M. Gabbouj, "Patient-specific seizure detection using nonlinear dynamics and nullclines," *IEEE J. Biomed. Health Informat.*, vol. 24, no. 2, pp. 543–555, Feb. 2020.
[46] S. Yuan, J. Liu, J. Shang, X. Kong, Q. Yuan, and Z. Ma, "The Earth mover's distance and Bayesian linear discriminant analysis for epileptic seizure detection in scalp EEG," *Biomed. Eng. Lett.*, vol. 8, no. 4, pp. 373–382, Nov. 2018.
[47] K. Tsiouris, S. Markoula, S. Konitsiotis, D. D. Koutsouris, and D. I. Fotiadis, "A robust unsupervised epileptic seizure detection methodology to accelerate large EEG database evaluation," *Biomed. Signal Process. Control*, vol. 40, pp. 275–285, Feb. 2018.
[48] R. S. Selvakumari, M. Mahalakshmi, and P. Prashalee, "Patient-specific seizure detection method using hybrid classifier with optimized electrodes," *J. Med. Syst.*, vol. 43, no. 5, pp. 1–7, May 2019.
[49] A. Bhattacharyya and R. B. Pachori, "A multivariate approach for patient-specific EEG seizure detection using empirical wavelet transform," *IEEE Trans. Biomed. Eng.*, vol. 64, no. 9, pp. 2003–2015, Sep. 2017.